

Dissipative particle dynamics simulations of electroosmotic flow in nano-fluidic devices

Duc Duong-Hong · Jian-Sheng Wang ·
G. R. Liu · Yu Zong Chen · Jongyoon Han ·
Nicolas G. Hadjiconstantinou

Received: 20 December 2006 / Accepted: 14 March 2007 / Published online: 17 April 2007
© Springer-Verlag 2007

Abstract When modeling the hydrodynamics of nano-fluidic systems, it is often essential to include molecular-level information such as molecular fluctuations. To this effect, we present a mesoscopic approach which combines a fluctuating hydrodynamics formulation with an efficient implementation of Electroosmotic flow (EOF) in the small Debye length limit. The resulting approach, whose major ingredient is Dissipative Particle Dynamics, is sufficiently coarse-grained to allow efficient simulation of the hydrodynamics of micro/nanofluidic devices of sizes that are too large to be simulated by ab initio methods such as

Molecular Dynamics. Within our formulation, EOF is *efficiently* generated using the recently proven similitude between velocity and electric field under appropriate conditions. More specifically, EOF is generated using an effective boundary condition, akin to a moving wall, thus avoiding evaluation of the computationally expensive electrostatic forces. Our method is used for simulating EOFs and DNA molecular sieving in simple and complex two-dimensional (2D) and 3D geometries frequently used in nano-fluidic devices. The numerical data obtained from our model are in very good agreement with theoretical results.

D. Duong-Hong (✉) · J.-S. Wang · G. R. Liu ·
Y. Z. Chen · J. Han · N. G. Hadjiconstantinou
Singapore–MIT Alliance, 9 Engineering Drive 1,
Singapore, Singapore 117576
e-mail: smadd@nus.edu.sg

J.-S. Wang
Department of Physics, National University of Singapore,
2 Science Drive 3, Singapore, Singapore 117542

G. R. Liu
Center for Advanced Computations in Engineering Science
(ACES), Department of Mechanical Engineering,
National University of Singapore, 9 Engineering Drive 1,
Singapore, Singapore 117576

Y. Z. Chen
Department of Pharmacy, National University of Singapore,
8 Science Drive 4, Singapore, Singapore 117543

J. Han
Department of Electrical Engineering and Computer Science,
Department of Biological Engineering, Massachusetts Institute
of Technology, Cambridge, MA 02139, USA

N. G. Hadjiconstantinou
Department of Mechanical Engineering, Massachusetts Institute
of Technology, Cambridge, MA 02139, USA

Keywords Computer simulation · Electroosmotic flows ·
Dissipative Particle Dynamics (DPD) method · MEMS ·
NEMS

1 Introduction

Electroosmotic flow (EOF) plays an important role in bio-hydrodynamics (hydrodynamics of flows containing biological molecules) in micro- and nano-fluidic devices (MEMS and NEMS) utilized for drug delivery, DNA separation and bio-sensors (Viovy 2000; Slater et al. 2002). Understanding the effects of EOF in microscale geometries is very important for facilitating better control and optimal design of such devices (Viovy 2000).

In general, the EOF profile can be obtained by solving the Navier–Stokes equations coupled with the Poisson–Boltzmann equation. Analytical solutions to those equations are possible for very simple cases (Smoluchowski 1903). However, numerical methods are needed for more complex geometries (Patankar and Hu 1998; Ermakov et al. 1998). Direct numerical simulation of EOF remains a

challenging task (Patankar and Hu 1998; Ermakov et al. 1998; Cummings et al. 2000) mainly due to the diverse range of scales of the problem from the Debye layer thickness (~ 1 nm) to the characteristic device lengthscale (usually > 10 μm). Also, these solutions cannot capture another important feature of the problem, namely molecular fluctuations (Brownian motion) of biomolecules, and their complicated, stochastic interaction with nanofluidic structures. Efficient protein separation has been demonstrated using regular nanofluidic filters (Fu et al. 2005, 2007) recently. For modeling and optimization of such devices, it would be critical to simulate both fluid flow (electroosmotic flow) and molecular fluctuation within the device, which is the source of molecular sieving (Fu et al. 2006).

Recently Kenward et al. (2003) and Tessier and Slater (2005) have used Molecular Dynamics (MD) to model the EOF in a narrow capillary. In those simulations, the charged particles are explicitly simulated. This method may provide an accurate solution for relatively small systems, but tends to become less effective for modeling typical micro/nano fluidic devices because of its high computational cost.

While mesoscopic techniques are more suitable for simulating such systems, effective numerical techniques are not yet available and implementation of such techniques has not been performed, partly because of the complexity of modeling EOF in these systems. As a result, in most of the recent simulation studies of micro fluidic systems, EOF has been neglected by assuming the presence of a high ionic strength buffer (Tessier et al. 2002; Streek et al. 2004). In this communication, we introduce a new method for generating EOF in arbitrary geometries with a mesoscopic technique, namely Dissipative Particle Dynamics (DPD). The computational cost of DPD is expected to be significantly lower than that of MD; at the same time, DPD can capture thermal fluctuations which are important for modeling a number of microscale phenomena, such as the entropic trapping in sieving devices (Viovy 2000; Slater et al. 2002) designed for biomolecule separation (Han and Craighead 2000; Tessier et al. 2002; Streek et al. 2004; Fu et al. 2005). Numerical results of previous DPD studies have been found to be consistent with available theoretical and experimental data (Cummings et al. 2000; Bow et al. 2006).

2 Theory on EOF

Electroosmotic flow refers to the fluid flow induced by the motion of the fluid in the charged Debye layer near a solid surface due to an external electric field applied along the surface. The interfacial charge may be formed by the

dissociation of chemical groups at the solid wall. For instance, a net negative surface charge is observed by the deprotonation of silanol groups at a silica-water interface (Tessier and Slater 2005). Counterions or ions subsequently accumulate from the solution into an electrical double layer near the surface. When an external electric field parallel to the surface is applied, the layer of mobile charges moves thereby “dragging” the bulk of the fluid via the action of viscosity.

In mean-field theory, the equilibrium distribution of mobile ions can be derived by the Poisson–Boltzmann equation which is established by combining the Poisson equation for the electrostatic potential $\psi(\mathbf{r})$ at position \mathbf{r} in the system with the Boltzmann distribution for the density of mobile ions in the solution in terms of the valence z_k and the bulk concentration n_k of each of the N species of ions (Viovy 2000):

$$\nabla^2 \psi = -\frac{e}{\epsilon_b \epsilon_0} \sum_{k=1}^N z_k n_k \exp(-e z_k \psi / k_B T), \quad (1)$$

where e is the magnitude of electron charge, k_B is the Boltzmann constant, T is temperature, and ϵ_0 , ϵ_b are the permittivity of vacuum and the dielectric constant of fluid, respectively.

In general, Eq. (1) can be solved numerically under appropriate boundary conditions, and the result is then substituted into the Navier–Stokes equation to obtain the resulting EOF field (Patankar and Hu 1998).

In this work, based on a recent study by Cummings et al. (2000), we develop a method that generates EOF in a DPD simulation in arbitrary geometries of practical interest without the need for solving Eq. (1) or directly computing electrostatic forces within the DPD formulation. This approach is valid in the limit that the Debye length,

$$\kappa^{-1} = \sqrt{\frac{\epsilon_b \epsilon_0 k_B T}{8\pi C e^2 z^2}}, \quad (2)$$

is small compared to the characteristic length-scale of a studied system. Here, C represents the ionic strength. As has been shown by Cummings et al. (2000), when this condition is satisfied and the flow is steady, fluid and electric properties are uniform and fluid velocities on all inlet and outlet boundaries satisfy

$$U_{\text{EOF}} = -\frac{\epsilon_b \epsilon_0 \zeta E}{\mu}, \quad (3)$$

the electric field and flow velocity are proportional, with the proportionality coefficient being constant throughout the domain. Here E is the local electric field, μ is the fluid viscosity and ζ is the zeta potential (Hunter 1981). Proof, as well

as an extensive discussion of the conditions of similitude can be found in the original paper of Cummings et al. (2000).

This relation allows one to generate the EOF field from the electric field (E), obtained by a solution of the Poisson equation. Once E is obtained, Eq. (3) can be used to supply an effective boundary condition to the DPD simulation. (Recall that the Debye layer is thin.) The resulting flow-field is guaranteed to be proportional (locally) to the electric field but also the correct EOF field. We use the former property (proportional to E) to test our implementation in Sect. 3.

3 A model of EOF and simulation results

3.1 A model of EOF

The DPD method describes the dynamical profiles of materials by simulating the motions of ensemble of particles or pseudo particles, and every particle is defined by its position, velocity and mass. Based on Newton’s equation of motion, the time evolution of the positions and velocities of DPD particles are calculated as follows,

$$\begin{aligned} \frac{d\mathbf{r}_i}{dt} &= \mathbf{v}_i, \\ \frac{d\mathbf{v}_i}{dt} &= \sum_{j \neq i} \mathbf{f}_{ij} + \mathbf{F}_e. \end{aligned} \tag{4}$$

Here, we assume the mass of particles is identical and normalized to unity; \mathbf{r}_i and \mathbf{v}_i are the position and the velocity vectors of particle i , respectively; \mathbf{F}_e is the external force; \mathbf{f}_{ij} is the inter-particle force exerted on particle i by particle j , consisting of three parts: conservative, dissipative and random (Hoogerbrugge and Koelman 1992).

The conservative force, \mathbf{F}_{ij}^C , is given by

$$\mathbf{F}_{ij}^C = \begin{cases} a_{ij}(1 - r_{ij}/r_c)\hat{\mathbf{r}}_{ij} & (r_{ij} < r_c), \\ 0 & (r_{ij} \geq r_c), \end{cases} \tag{5}$$

where a_{ij} is the maximum repulsion between particles i and j , $\mathbf{r}_{ij} = \mathbf{r}_i - \mathbf{r}_j$, $r_{ij} = |\mathbf{r}_{ij}|$, $\hat{\mathbf{r}}_{ij} = \mathbf{r}_{ij}/r_{ij}$ is the unit vector directed from particle j to i , and r_c is a cut-off radius, here normalized to unity.

The dissipative force, \mathbf{F}_{ij}^D , and the random force, \mathbf{F}_{ij}^R , are given by

$$\mathbf{F}_{ij}^D = -\gamma\omega^D(r_{ij})(\hat{\mathbf{r}}_{ij} \cdot \mathbf{v}_{ij})\hat{\mathbf{r}}_{ij}, \tag{6}$$

and

$$\mathbf{F}_{ij}^R = \sigma\omega^R(r_{ij})\theta_{ij}\hat{\mathbf{r}}_{ij}, \tag{7}$$

respectively, where $\mathbf{v}_{ij} = \mathbf{v}_i - \mathbf{v}_j$, and γ and σ are the coefficients characterizing the strengths of the dissipative

and random forces, ω^D and ω^R are the weight functions that vanish if $r_{ij} \geq r_c$, and θ_{ij} is white noise with the properties:

$$\langle \theta_{ij}(t) \rangle = 0 \text{ and } \langle \theta_{ij}(t)\theta_{kl}(t') \rangle = (\delta_{ik}\delta_{jl} + \delta_{il}\delta_{jk})\delta(t - t'). \tag{8}$$

To satisfy the detailed balance, the weight functions obey a relation similar to the fluctuation-dissipation theorem,

$$\omega^D(r_{ij}) = [\omega^R(r_{ij})]^2 \text{ and } \gamma = \frac{\sigma^2}{2k_B T}, \tag{9}$$

where $k_B T$ is the Boltzmann temperature. The weight function is calculated by:

$$\omega^D(r_{ij}) = [\omega^R(r_{ij})]^2 = \begin{cases} \sqrt{1 - r_{ij}/r_c} & r_{ij} < r_c, \\ 0 & r_{ij} \geq r_c. \end{cases} \tag{10}$$

The equations of motion (4) are solved by using the velocity-Verlet algorithm suggested by Groot and Warren (1997). The DPD parameters are calculated based mostly on the previous works of Groot and Warren (1997) and Duong-Hong et al. (2004) and listed in Table 1.

As described above, the velocity profile of EOF can be obtained by using Eq. (3) as a boundary condition. To do this, we compute the electric field in the computational domain (regions covered by a simulation study) by directly solving the Laplace equation subject to von Neumann boundary condition at the walls, followed by the computation of the electrostatic velocity at the wall, \mathbf{U}_{wall} , (in reality a Debye length from the wall) by using Eq. (3) and the previously computed electric field and the given zeta potential. In our case, ζ was approximated by the following relation (Pennathur and Santiago 2005):

$$\zeta = 0.0288C^{-0.245}, \tag{11}$$

which is again confirmed by the experimental data of Bow et al. (2006), where C represents ionic strength measured in moles/liter, and ζ is the zeta potential in mV.

The velocity, \mathbf{U}_{wall} , is locally assigned to the wall particles; the ‘‘moving wall’’ then drags the fluid particles by viscosity. It is important to note that the position of wall

Table 1 The DPD parameters

Parameters	DPD value
$k_B T$	1.0
a_{ij} (between fluid-fluid particles)	75.0
a_{ij} (between fluid and wall particles)	8.66
σ (for all particles)	3.0
r_c	1.0

particles is not updated (i.e. they are effectively “frozen”); rather, the kinematic information about the motion of the wall particles is transferred to the fluid particles by the interaction forces in DPD and the bounce-back boundary condition described below which takes the wall motion into account.

In DPD, due to the ‘soft’ repulsive force, particles sometimes penetrate the wall and exit the computational domain. To prevent this from occurring we apply a double layer wall structure (Duong-Hong et al. 2004), as well as a bounce-back boundary condition (Willemsen et al. 2000) for particles which penetrate the wall. This condition serves as a no-slip boundary condition and amounts to resetting the positions and velocities of particles exiting the domain to the new values given by Eqs. (12) and (13), respectively. The new position of a particle crossing the wall is given by

$$\mathbf{r}_{\text{new}} = \mathbf{r}_{\text{old}} + 2d_r \mathbf{n}_w, \quad (12)$$

and the new velocity is given by

$$\mathbf{v}_{\text{new}} = 2\mathbf{U}_{\text{wall}} - \mathbf{v}_{\text{old}}, \quad (13)$$

where d_r normal distance the particle has penetrated into the boundary from a particle which is outside the computational domain and \mathbf{n}_w is the normal vector on the wall pointing into the simulation domain; \mathbf{U}_{wall} is the velocity of the wall. Equations (12) and (13) have been shown to effectively model the no-slip boundary condition for both static wall and moving wall (Duong-Hong et al. 2004).

3.2 Simulation results

Simulations were performed in two-dimensional (2D) and 3D channels of non-dimensional size 100×100 and $100 \times 100 \times 5$, respectively; as the density of solvent particles is chosen to be 1.0, resulting in 10,000 and 50,000 particles in the 2D and 3D channels, respectively. Non-dimensional quantities are constructed using the length unit $[\sigma] = 18 \text{ nm}$, the mass unit $[\mathbf{m}] = 5 \times 10^{-15} \text{ kg}$, and the energy unit $[\epsilon]: 300k_B T = 4.14 \times 10^{-21} \text{ J}$. The time unit $[\mathbf{t}]$ directly follows from the above and is equal to $(\sqrt{\mathbf{m}\sigma^2/\epsilon}) \sim 1.98 \times 10^{-5} \text{ s}$. These units are chosen so that the shear viscosity of the fluid can be comparable with that of water; such mesoscale units allow modeling of various systems with length scales ranging from nanometers to micrometers and overall time scales up to several seconds.

The channels are defined by walls in the y direction; periodic boundary conditions are applied in the other directions. The density and the viscosity of solvent are $1,000 \text{ kg m}^{-3}$ and $9 \times 10^{-4} \text{ Pa s}$, respectively. The ionic strength is C ($\sim 5 \times \text{TBE}$) and the electric field is

100 V cm^{-1} along the channel axis (x -direction). The non-dimensional velocity of EOF is then calculated to be $\mathbf{U}_{\text{wall}} = (0.325, 0, 0) = (U_{\text{wall}}, 0, 0)$. We assume that the electric potential is steady and constant everywhere within the channel (and that the Debye length, of which the maximum thickness is $\sim 10 \text{ nm}$ as calculated by Eq. (2) with $z = 1$, or 3.8 nm as reported in the experiment of Bow (2006), is much smaller than the channel width $\sim 1.8 \mu\text{m}$). The electroosmotic velocity profile in this case is expected to be plug-like as shown in Fig. 1.

Figure 1 shows that the fully developed velocity profile is in excellent agreement with the prediction of Eq. (3). Note that the difference between the cases of Debye length of 1.8 and 10 nm is within the statistical uncertainty of our calculations.

Our next validation example is motivated by recent experiments on DNA separation systems (Han and Craighead 2000). We chose a channel geometry very similar to the actual experiments, namely a series of deep and shallow channels (T-channel in short). Cummings et al. (2000) have performed experiments of EOF in a similar T-shaped channel and confirmed the similitude between the EOF velocity and the electric field.

The channel dimensions are (100,25) in 2D and (100,25,5) in 3D, respectively (see Fig. 2). As the conditions for similitude between the fluid velocity and electric field in EOF still hold in our simulations, a direct comparison between the velocities calculated by Eq. (3) at the same previous conditions and the velocities obtained from our simulations is used to validate the method.

We simulated 5×10^6 time steps; the velocity is averaged in a grid of bins (500×125 bins in x and y direction, respectively) and averaged over the last 2×10^5 time steps (the calculations being done on a single-processor desktop

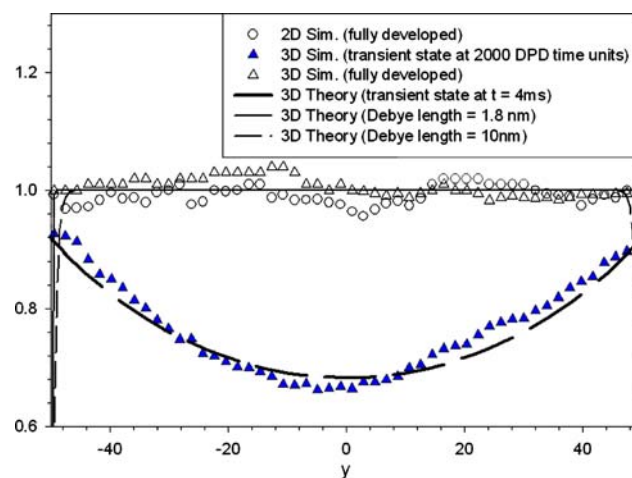


Fig. 1 The transient and fully developed “plug-flow” velocity profile of EOF in 2D and 3D planar channels compared with the theoretical results for the cases of different Debye lengths

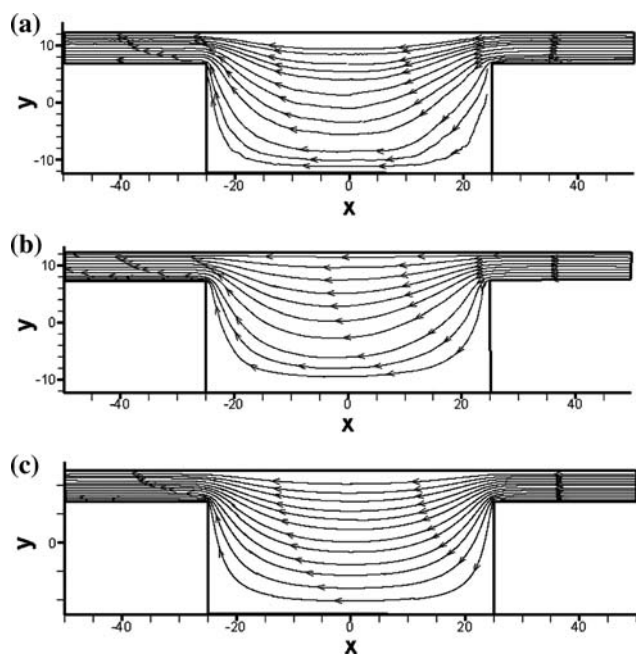


Fig. 2 A comparison between the streamlines of simulation results in 2D- (a) and 3D-T-channel (b) with the theoretical result (c)

computer). In Fig. 2, the resulting streamlines are shown to be very similar to the theoretical results. The result of 3D-simulation appears smoother and closer to the theoretical result than that of 2D-simulation. It is simply because in the 3D-simulation the number of samples increases by the additional particles in the z direction that leads to better averaging result.

Figure 3 provides a more detailed comparison: the components of the longitudinal velocity distribution at particular positions of the channel, e.g. $x = -40$, $x = 0$, and $x = 20$ are compared to the theoretical result. This figure shows that the components of velocity at different positions in the T-channel are in good agreement with the theoretical results for both 2D and 3D simulations. Particularly, in the constriction area of T-channel, the EOF velocity, shown in Fig. 3a, is of plug-flow profile as expected. In addition, we have also simulated some larger channels in both 2D and 3D cases (lengths up to $10 \mu\text{m}$) and the results are again consistent with the theoretical ones but they are not shown here in the sake of brevity.

The results obtained so far confirm the ability of our model to simulate EOF in both simple and complex channels. A nice feature of the DPD simulation is the ability to track particle movement. A typical path of a particle in the electrophoretic flow is tracked and shown in Fig. 4. It clearly demonstrates the fluctuating nature of molecular motion. This is important because in most filtration processes involving biological molecules, such as Ogston sieving process, fluctuations are very important and must be considered (Fu et al. 2006).

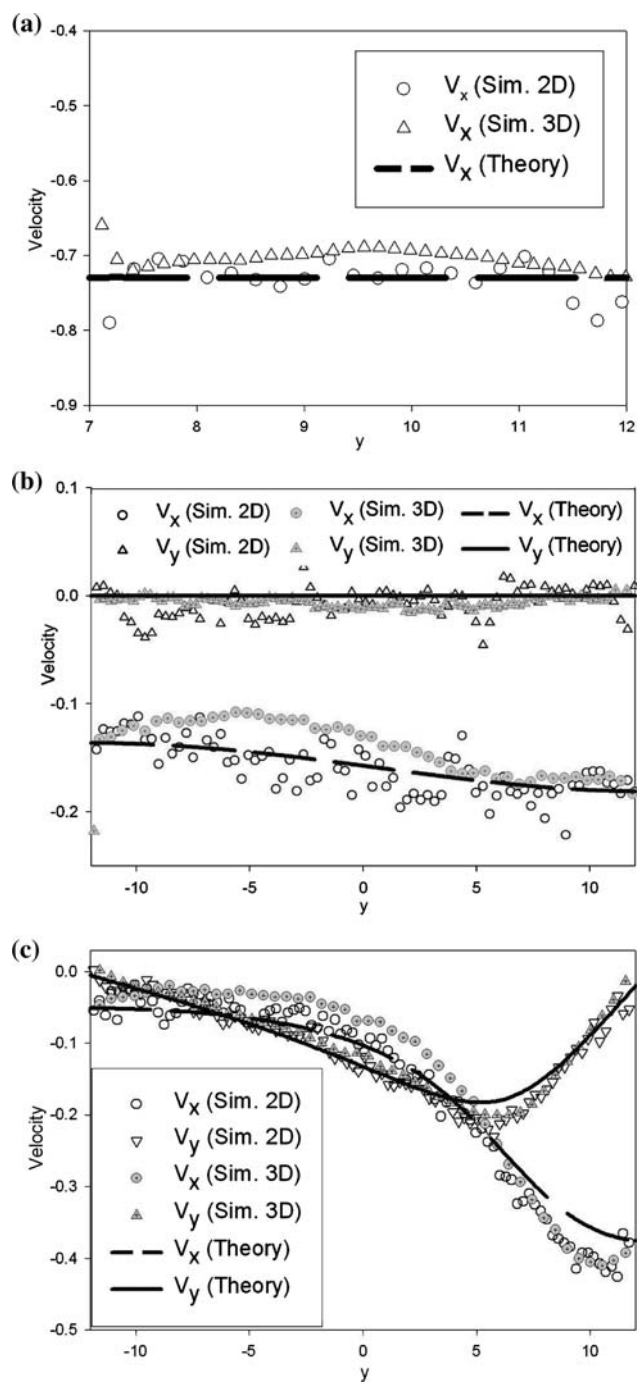


Fig. 3 A comparison of longitudinal velocity components of our simulations (2D and 3D) with the theoretical results at different positions in T-channel: **a** $x = -40$; **b** $x = 0$; and **c** $x = 20$

With this in mind, we also investigate the motion of a polymer chain modeled by a set of 40 beads connected by a worm-like spring force (Shaqfeh 2005)

$$\mathbf{F}_{ij}^w = -\frac{k_B T}{4P} \left[\left(1 - \frac{r_{ij}}{l}\right)^{-2} + \frac{4r_{ij}}{l} - 1 \right] \hat{\mathbf{r}}_{ij} \quad (14)$$

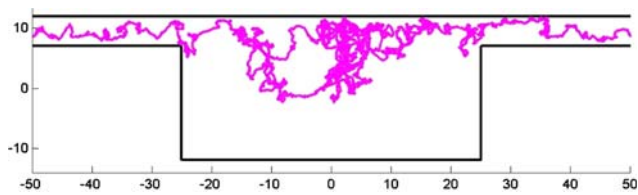


Fig. 4 A typical path of a fluid particle in EOF in T-channel

where r_{ij} is the distance of bead i and j , l is the maximum length of one chain segment and P is the effective persistence length of the chain. In the wormlike model, the persistence length is typically chosen to be 50 nm for modeling a standard DNA chain (Nkodo et al. 2001). The polymer chain in this simulation is regarded as an uncharged DNA chain. The maximum segment length is chosen to be 2.547; in other words, the chain of 40 beads models a 5.37 kbp DNA.

The diffusion of the DNA chain is first investigated by simulating a DNA chain in a sea of the above solvent. The chain is suspended in a large channel ($500 \times 100 \times 100$) and periodic boundary conditions are applied in all directions. The diffusion of the chain is found to be about $1.22 (\times 10^{-9} \text{ cm}^2 \text{ s}^{-1})$ which is comparable with $1.10 (\times 10^{-9} \text{ cm}^2 \text{ s}^{-1})$ for the 4.7 kbp dsDNA from the experimental data of Nkodo (2001). Notice again that the chain is considered as an uncharged polymer chain to separate the electrophoretic effect.

Figure 5 shows a path of a polymer-chain particle in EOF in a T-channel; it again demonstrates the fluctuating nature of the motion of this particle. In this particular example, the chain particle is trapped in the deep well ($\sim 6,530 [t]$) longer than the fluid particles ($\sim 1,720 [t]$). Consequently, the average velocity of the chain particle ($\sim 0.025 [\sigma/t]$) is much smaller than that of the fluid particles ($\sim 0.092 [\sigma/t]$). The above results have confirmed that the stochastic motion of fluid/analyte molecules in water, as well as their interaction with the nanofluidic structures, can be captured using DPD simulations, allowing us to better understand sieving processes such as Ogston sieving (Fu et al. 2006) in more microscopic terms.

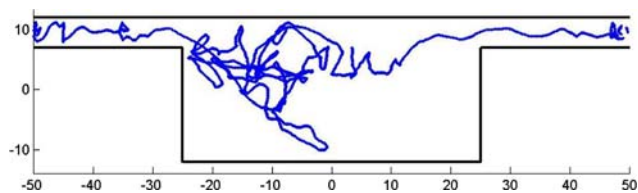


Fig. 5 A typical path of a chain particle flowing in EOF in T-channel. Symbol is placed at the center of mass of the chain particle. The chain particle is hindered from entering nanochannel for some time, before eventually entering the nanochannel

Moreover, our approach is expected to be straightforwardly extendable to transient flows since it appears plausible that the effective boundary condition approach will hold in the case that the hydrodynamic evolution timescale is long compared to the timescale of evolution of the electric field, leading to a purely hydrodynamic problem. The DPD method can capture the transient development of such flows provided the characteristic timescale $[t]$ is significantly smaller than the characteristic evolution time of the transient flow. This latter time for the geometries studied here is given (approximately) by $\frac{D^2 \rho}{\mu} \sim 10^{-5} \text{ s}$ (Yan et al. 2006) where D is the characteristic length-scale of the cross section. This suggests that $[t]$ needs to be reduced before transient flows of these dimensions can be accurately captured.

4 Conclusions

In summary, we have presented a mesoscopic technique capable of modeling EOF in arbitrary geometries for the case of thin Debye layer. However, if the thickness of the Debye layer is comparable to the width of the channel, the technique cannot provide a detailed description of shear flow within the thickness of the Debye layer. In the limit of thin Debye layer, the technique is validated for both simple planar and complex (deep and shallow) channels. This technique is easy to implement and computationally efficient (all simulations presented here were performed on a single-processor desktop computer). It represents one step forward towards the simulation of complex biohydrodynamics in NEMS and MEMS devices of practical interest.

Acknowledgments This study is funded by the Singapore-MIT Alliance.

References

- Bow HC (2006) Characterization of nanofilter arrays for small molecule separation. Master thesis for Masters of Science in Electrical Engineering and Computer Science at the Massachusetts Institute of Technology
- Cummings EB, Griffiths SK, Nilson RH, Paul PH (2000) Conditions for similitude between the fluid velocity and electric field in electroosmotic flow. *Anal Chem* 72:2526–2532
- Duong-Hong D, Phan-Thien N, Fan XJ (2004) An implementation of no-slip boundary conditions in DPD. *Comput Mech* 35:24–29
- Ermakov SV, Jacobson SC, Ramsey JM (1998) Computer simulations of electrokinetic transport in microfabricated channel structures. *Anal Chem* 70:4494–4504
- Fu J, Mao P, Han J (2005) A nanofilter array chip for fast gel-free biomolecule separation. *Appl Phys Lett* 87(1–3):263902
- Fu J, Yoo J, Han J (2006) Molecular sieving in periodic free-energy landscapes created by patterned nanofilter arrays. *Phys Rev Lett* 97(1–4):018103

- Fu J, Schoch RR, Stevens AL, Tannenbaum SR, Han J (2007) Patterned anisotropic nanofluidic sieving structure for continuous-flow separation of DNA and protein. *Nat Nanotechnol* 2:121–128
- Groot RD, Warren PB (1997) Dissipative particle dynamics: bridging the gap between atomic and mesoscopic simulation. *J Chem Phys* 107(11):4423–4435
- Han J, Craighead HG (2000) Separation of long DNA Molecules in a microfabricated entropic trap array. *Science* 288:1026–1029
- Hoogerbrugge PJ, Koelman JMVA (1992) Simulating microscopic hydrodynamic phenomena with dissipative particle dynamics. *Europhys Lett* 19(3):155–160
- Hunter RJ (1981) *Zeta potential in colloid science: principles and applications*. Academic, New York
- Kenward M, Tessier F, Tatk Y, Gratton Y, Guillouzie S, Slater GW (2003) Molecular dynamics simulation of polymers in micro-environments. <http://hpcs2003.ccs.usherbrooke.ca/papers/Kenward.pdf>
- Nkodo AE, Garnier JM, Tinland B, Ren H, Desruisseaux C, McCormick LC, Drouin G, Slater GW (2001) Diffusion coefficient of DNA molecules during free solution electrophoresis. *Electrophoresis* 22:2424–2432
- Patankar NA, Hu HH (1998) Numerical simulation of electroosmotic flow. *Anal Chem* 70:1870–1881
- Pennathur S and Santiago JG (2005) Electrokinetic transport in nanochannels. 2. Experiments. *Anal Chem* 77:6782–6789
- Shaqfeh ESG (2005) The dynamics of single-molecule DNA in flow. *J N-N Fluid Mech* 130:1–28
- Slater GW, Guillouzie S, Gauthier MG, Mercier J-F, Kenward M, McCormick LC, Tessier F (2002) Theory of DNA electrophoresis (~1999–2002 1/2). *Electrophoresis* 23:3791–3816
- Smoluchowski M Von (1903) Contribution a' la théorie de l'endosmose électrique et de quelques phénomènes corrélatifs. *Bull Int Acad Sci Cracovie* 8:182–200
- Streek M, Schmid F, Duong TT, Ros A (2004) Mechanisms of DNA separation in entropic trap arrays: a Brownian dynamics simulation. *J Biotech* 112:79–89
- Tessier F, Slater GW (2005) Control and quenching of electroosmotic flow with end-grafted polymer chains. *Macromolecules* 38:6752–6754
- Tessier F, Labrie J, Slater GW, (2002) Electrophoretic separation of long polyelectrolytes in submolecular-size constriction: a Monte Carlo study. *Macromolecules* 35:4791–4899
- Violy JL (2000) Electrophoresis of DNA and other polyelectrolytes: physical mechanisms. *Rev Mod Phys* 73(3):813–872
- Willemsen SM, Hoefsloot HCJ, Iedema PD (2000) No-slip boundary condition in dissipative particle dynamics. *Int J Mod Phys C* 11(5):881–890
- Yan D, Nguyen NT, Yang C, Huang X (2006) Visualizing the transient electroosmotic flow and measuring the zeta potential of microchannels with a micro-PIV technique. *J Chem Phys* 124(1–4):021103